Electronic Supplementary Information (ESI)

For

Structural, spectroscopic, and electrochemical properties of tri- and tetradentate N_3 and N_3S Copper complexes with mixed benzimidazole/thioether donors

Ivan Castillo,*[†] Víctor M. Ugalde-Saldívar,[‡] Laura A. Rodríguez Solano,[†] Brenda N. Sánchez Eguía,[†] Erica Zeglio,[§] Ebbe Nordlander[§]

[†]*Instituto de Química, Universidad Nacional Autónoma de México, Circuito Exterior, Ciudad Universitaria, México, D. F., 04510, México.*

[‡]*Facultad de Química, División de Estudios de Posgrado, Universidad Nacional Autónoma de México, Ciudad Universitaria, México, D. F., 04510, México.*

[§]*Inorganic Chemistry Research Group, Chemical Physics, Center for Chemistry and Chemical Engineering, Lund University, Box 124, SE-221 00 Lund, Sweden.*

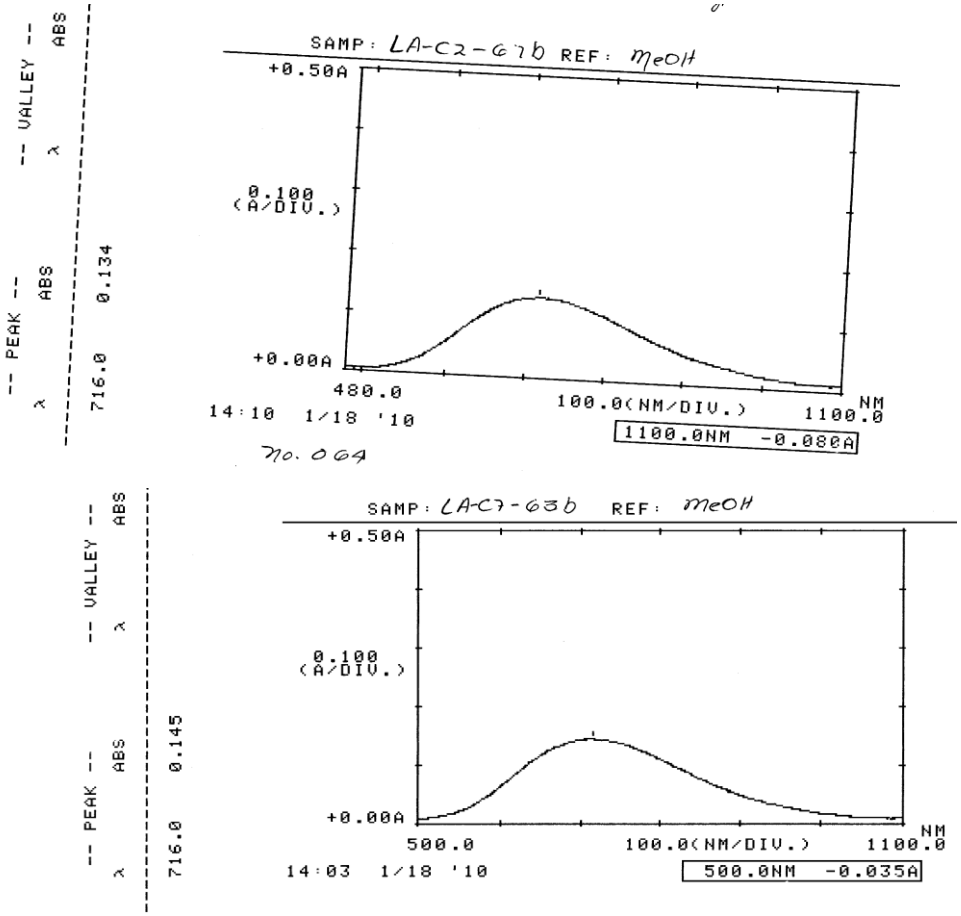

Figure S1. UV-vis spectra of complexes **1** and **2**.

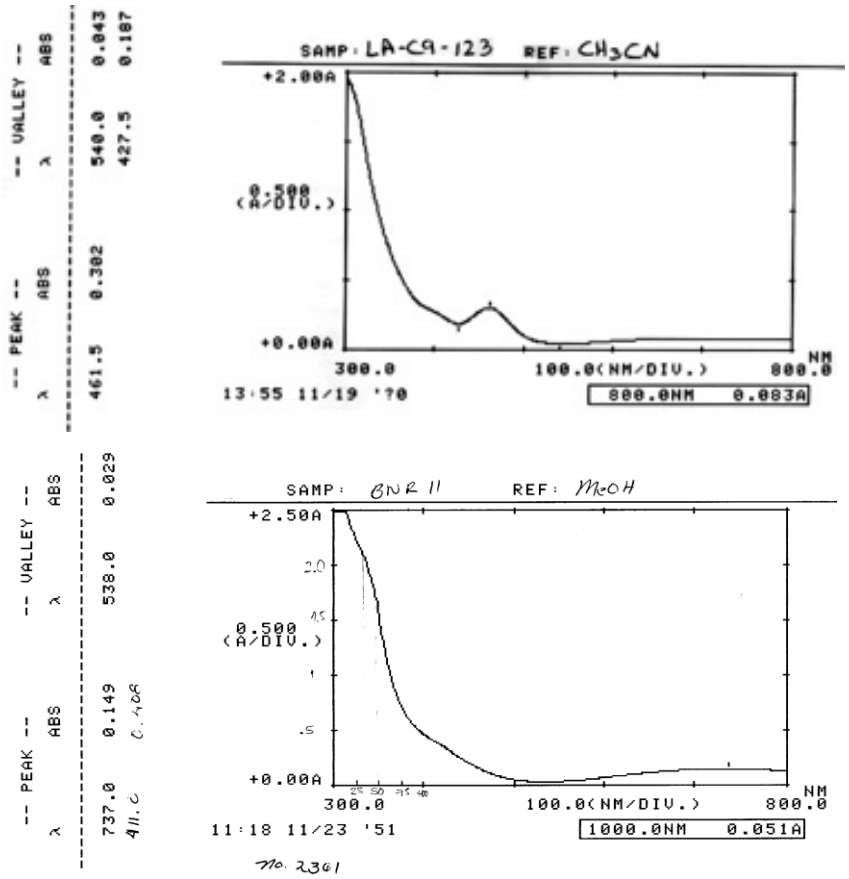

Figure S2. UV-vis spectra of complexes **3** and $\mathbf{3^{Me}}$.

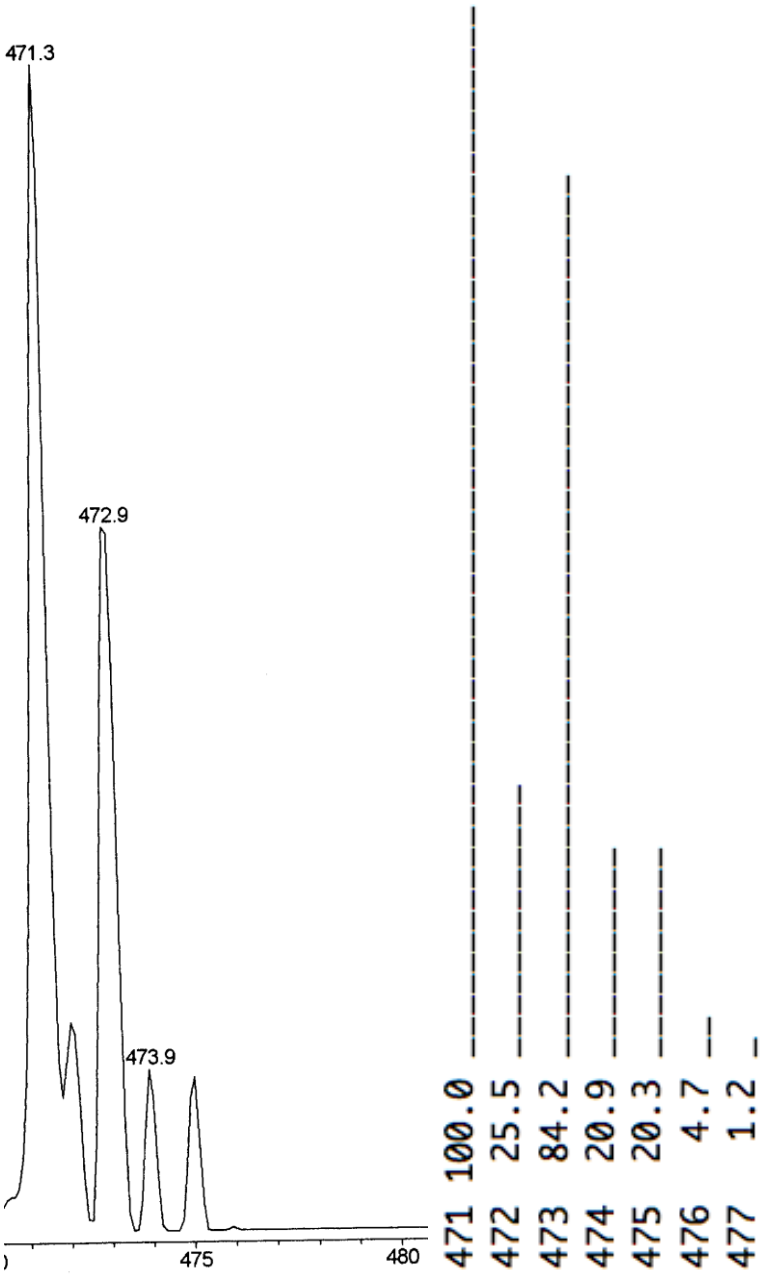

Figure S3. ESI-MS of complex **1** and simulation with isotopic pattern.

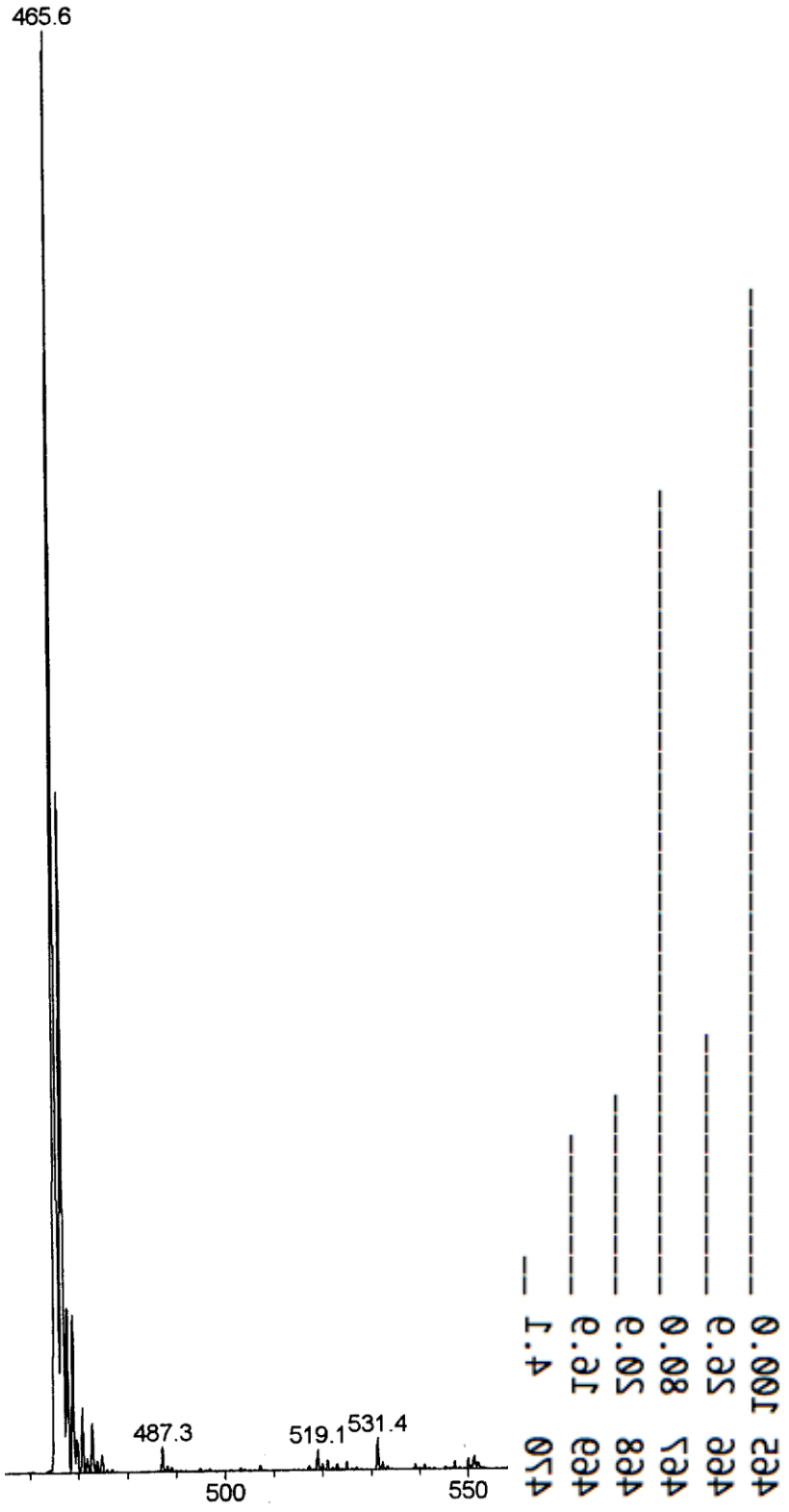

Figure S4. ESI-MS of complex **2** and simulation with isotopic pattern.

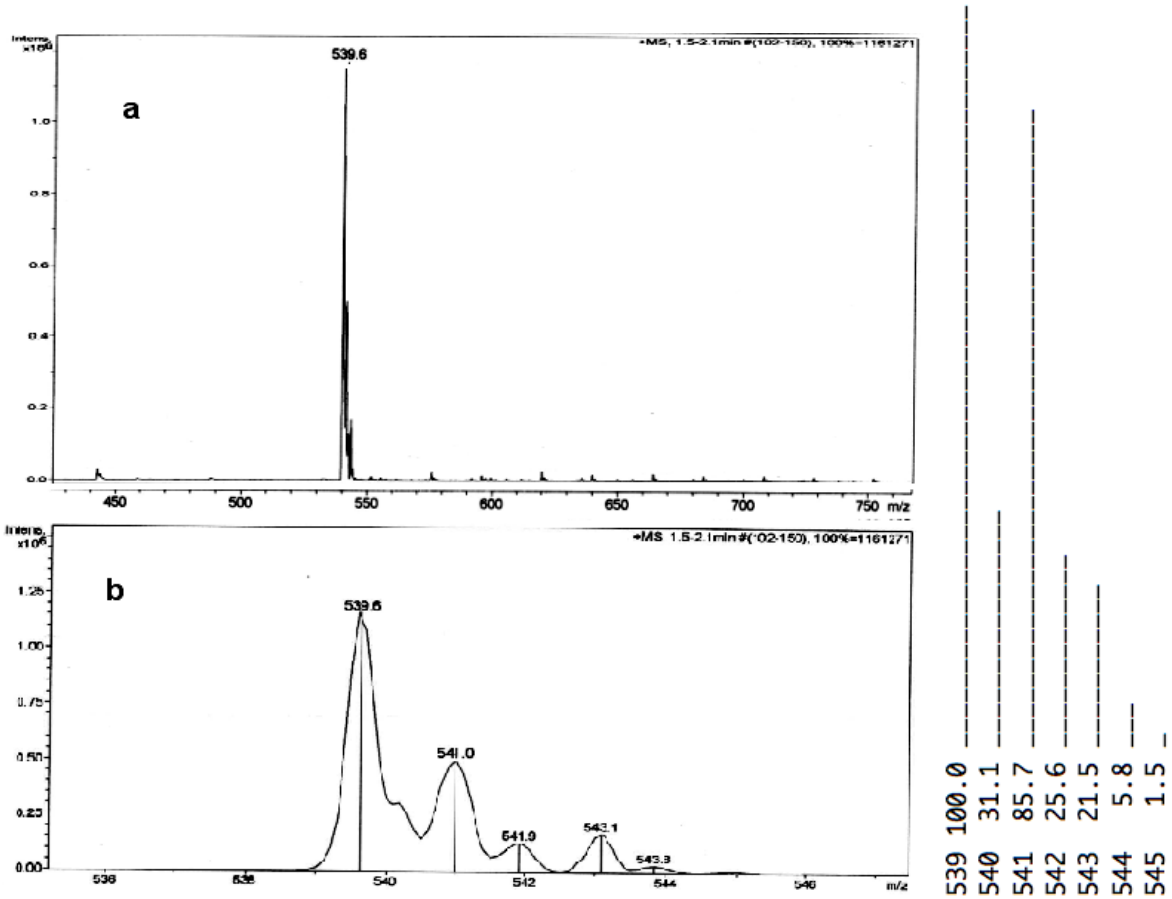

Figure S5. ESI-MS of complex **3** and simulation with isotopic pattern.

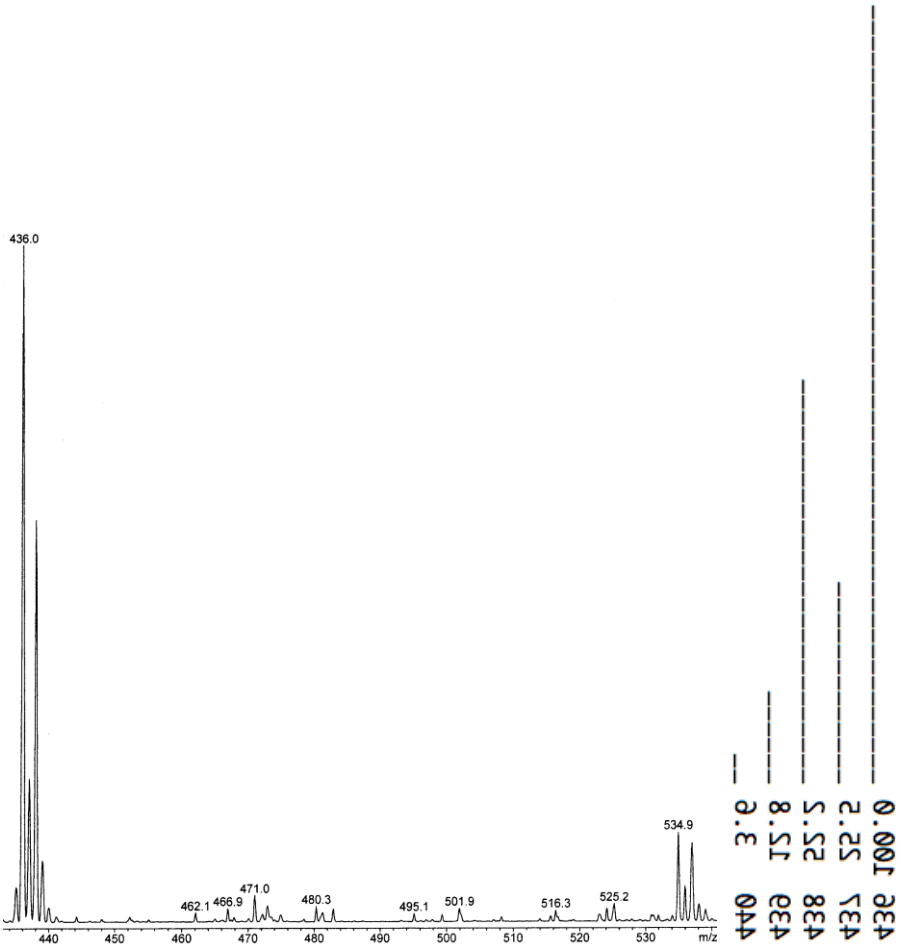

Figure S6. ESI-MS of complex **4** and simulation with isotopic pattern.

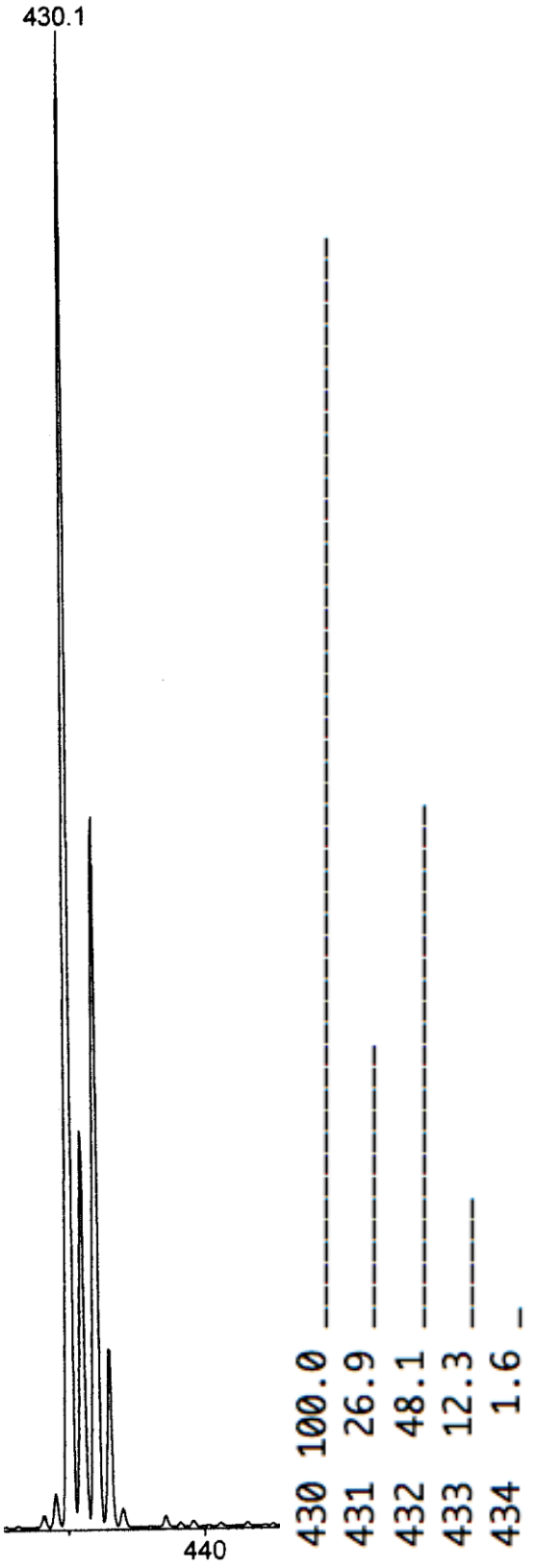

Figure S7. ESI-MS of complex **5** and simulation with isotopic pattern.

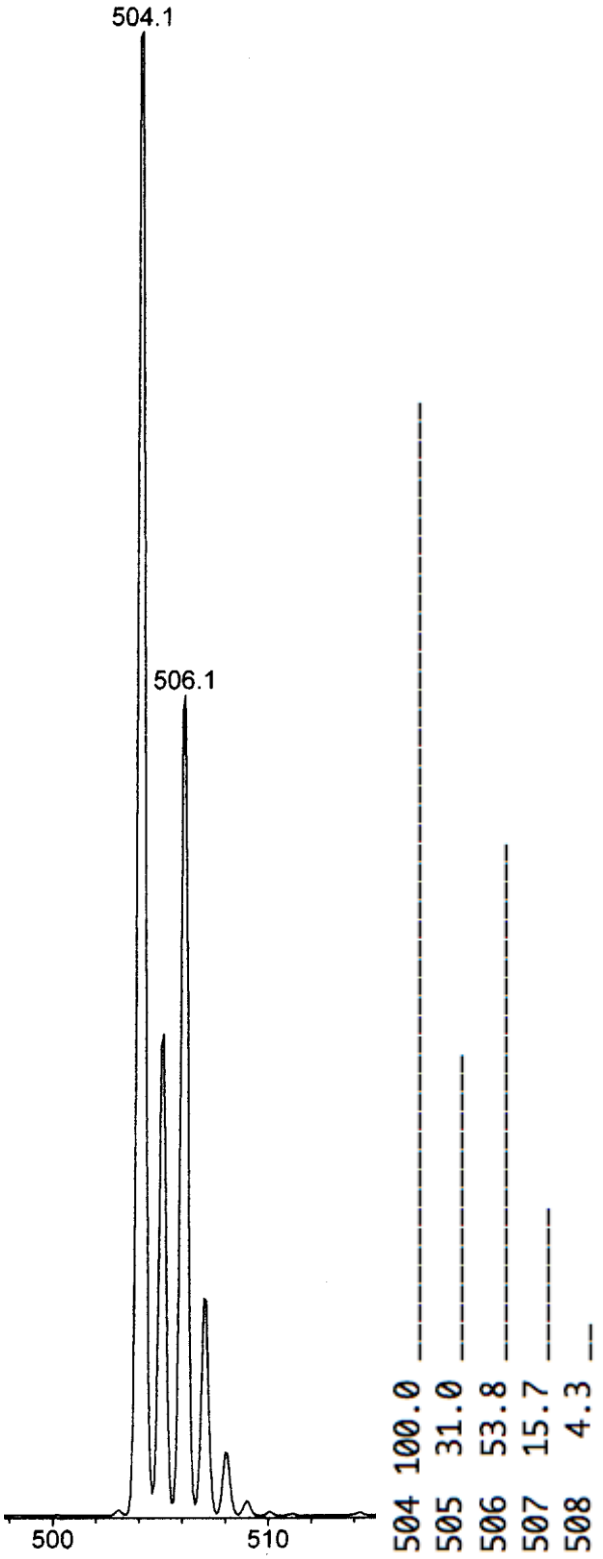

Figure S8. ESI-MS of complex **6** and simulation with isotopic pattern.

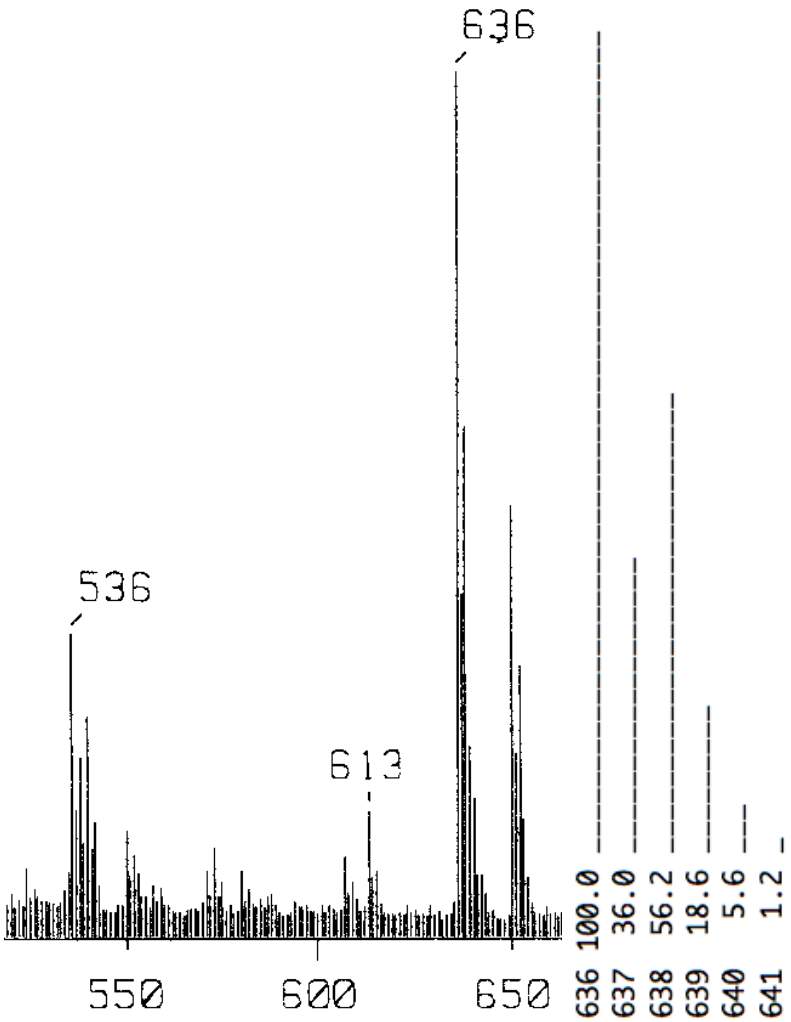

Figure S9. FAB-MS of complex **4**$^{\mathbf{BOC}}$ and simulation with isotopic pattern.

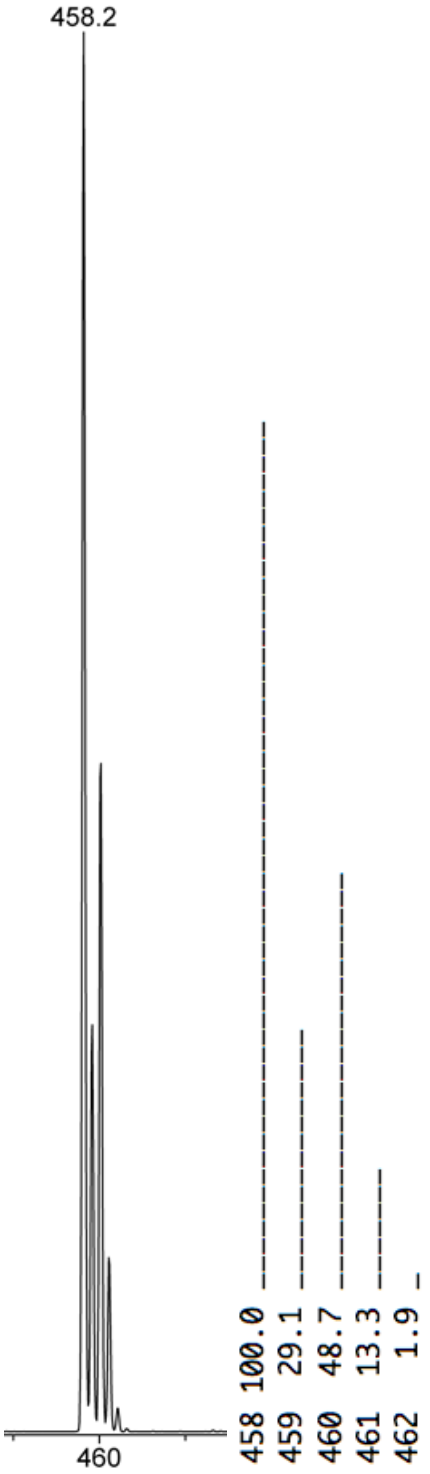

Figure S10. ESI-MS of complex $\mathbf{5}^{\mathbf{Me}}$ and simulation with isotopic pattern.

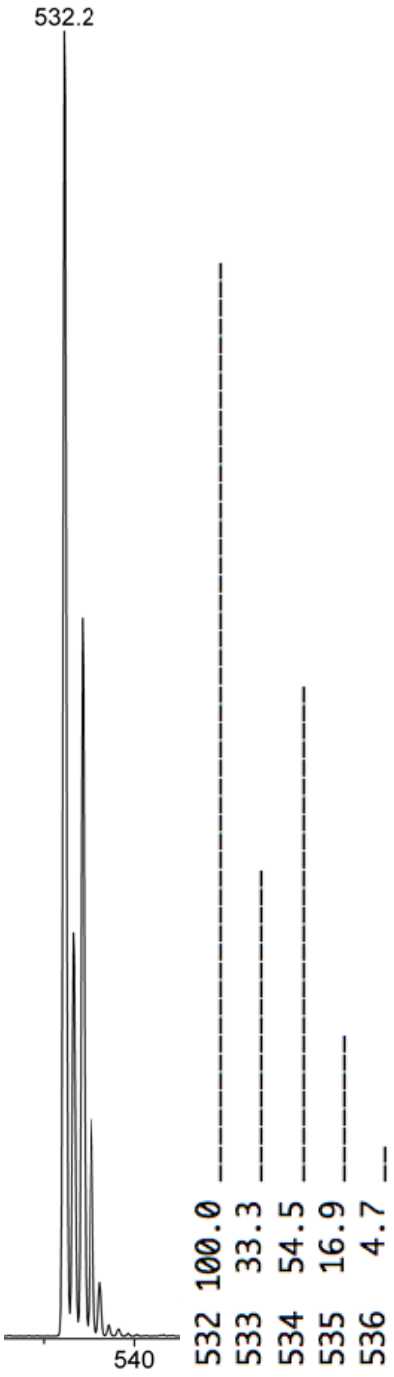

Figure S11. ESI-MS of complex $\mathbf{6}^{\mathbf{Me}}$ and simulation with isotopic pattern.

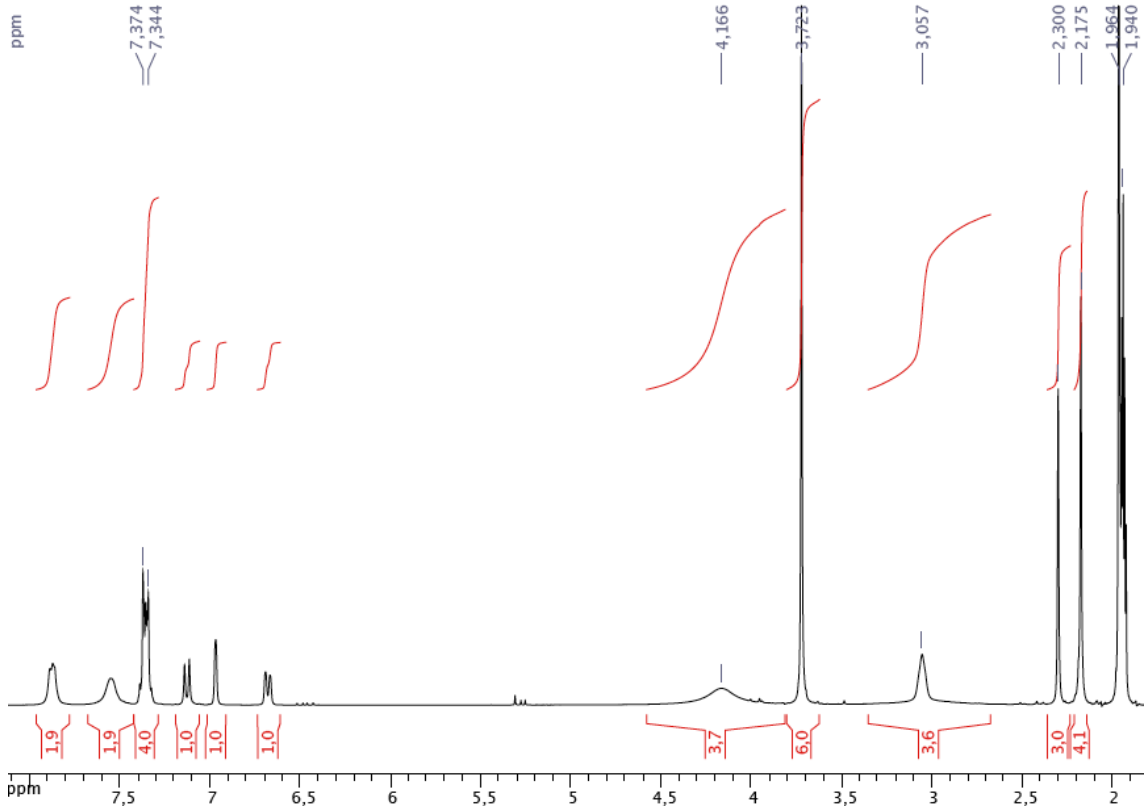

Figure S12. ^{1}H NMR spectrum of complex **6**$^{\mathbf{Me}}$ in CD_3CN.

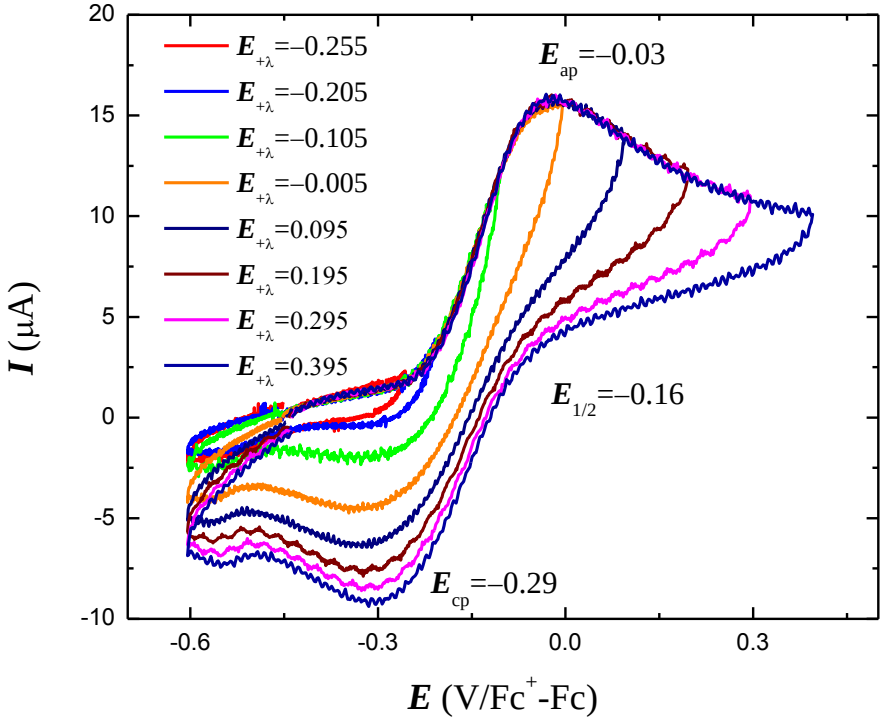

Figure S13. Representative cyclic voltammograms of 1 mM solutions of complex **6**$^{\mathbf{Me}}$ in 0.1 M Bu_4NPF_6 in acetonitrile, at different inversion potential values.

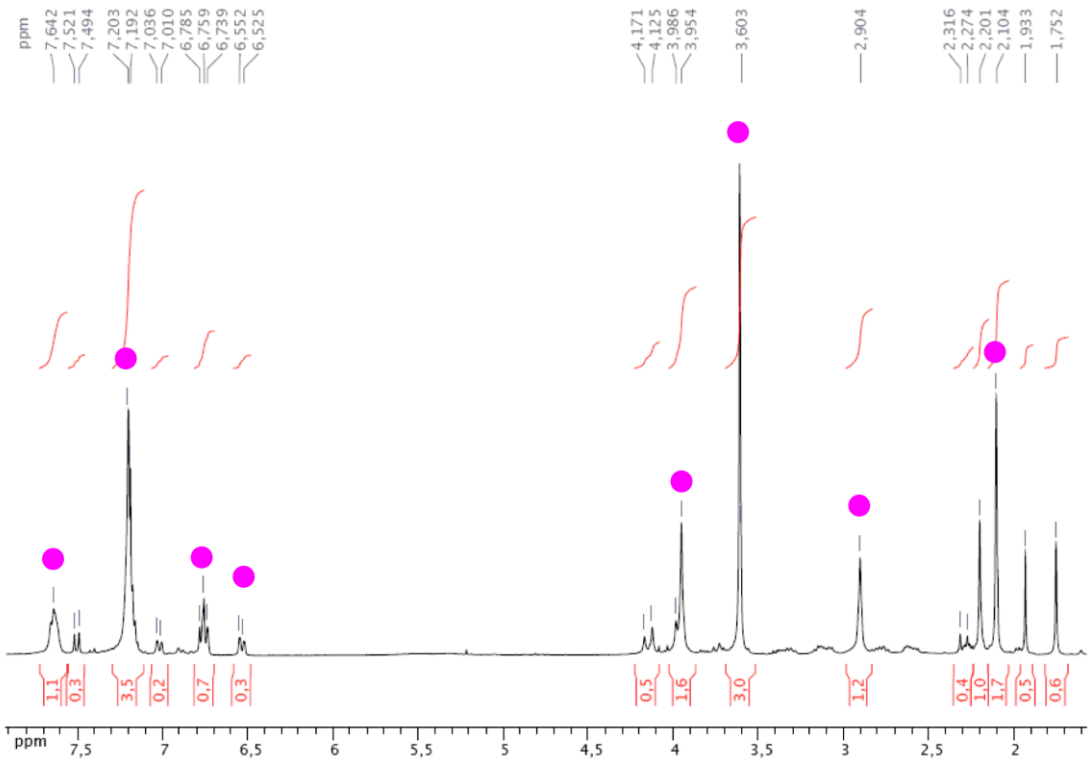

Figure S14. ^{1}H NMR spectrum of the ligand-oxidation products of $\mathbf{6^{Me}}$ in $CDCl_3$; resonances marked with a pink circle correspond to ligand $\mathbf{Me_2L^3}$.

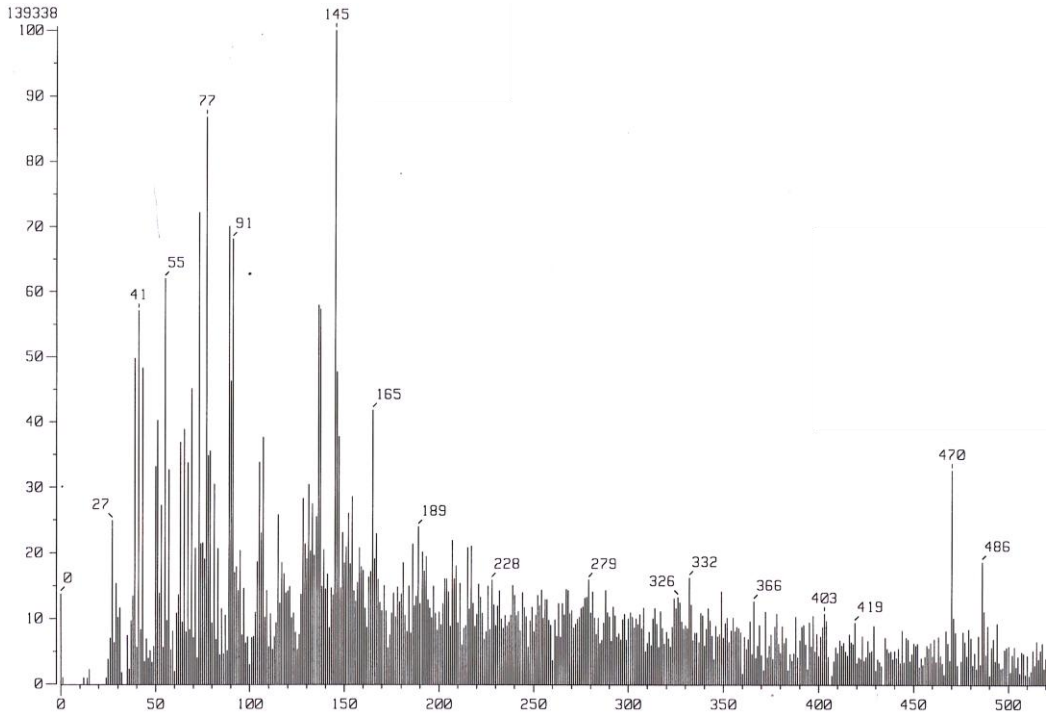

Figure S15. FAB-MS of the ligand-oxidation products of $\mathbf{6^{Me}}$, the peak at *m/z* = 470 corresponds to ligand $\mathbf{Me_2L^3}$.

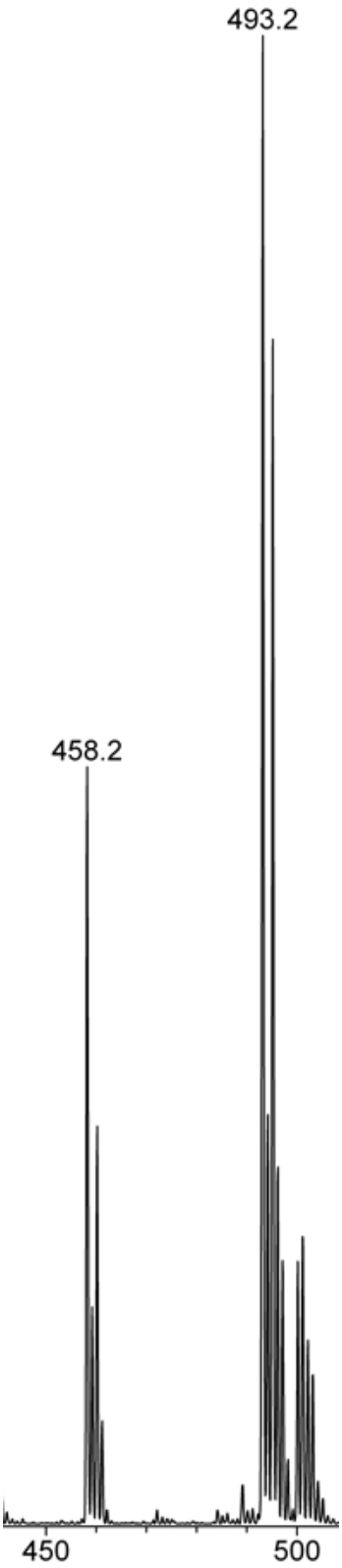

Figure S16. ESI-MS spectrum of $\mathbf{5}^{\mathbf{Me}}$ after exposure to O_2 in acetonitrtile solution.

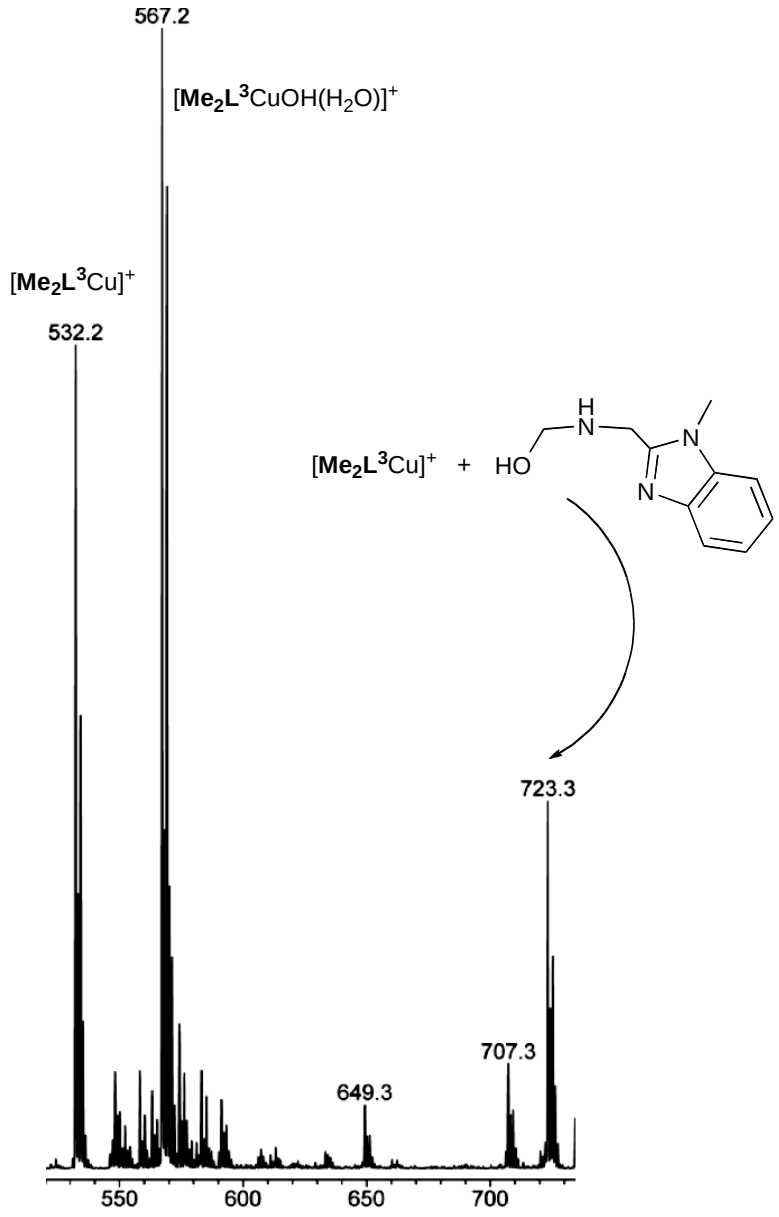

Figure S17. ESI-MS of the oxygenation products of **6**$^{\mathbf{Me}}$ in acetonitrile.

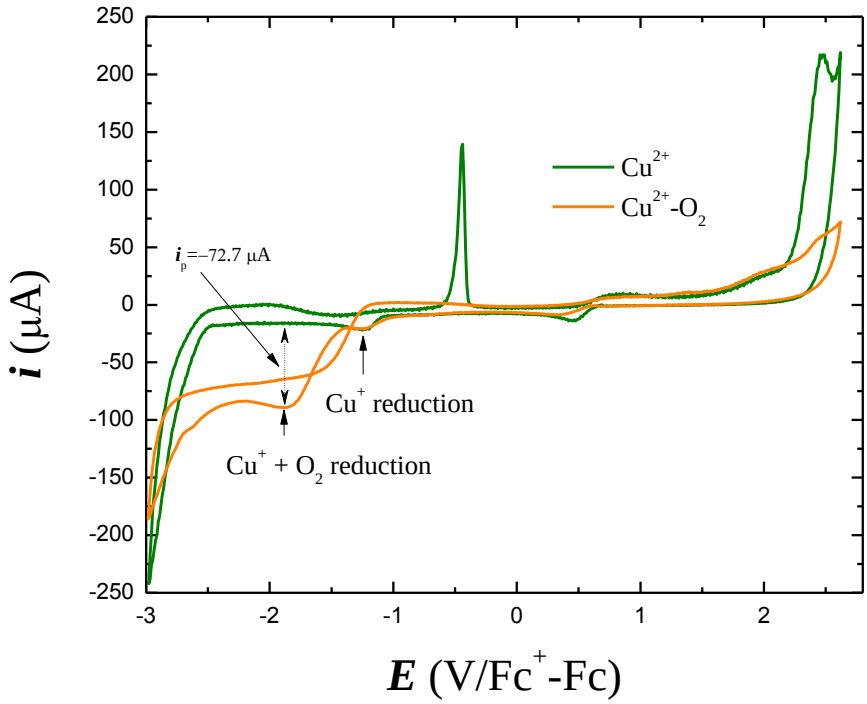

Figure S18. Representative voltammogram of 1 mM acetonitrile solution of $Cu(NO_3)_2$ at –13°C: under N_2 atmosphere (green line), in the presence of O_2 (yellow line).

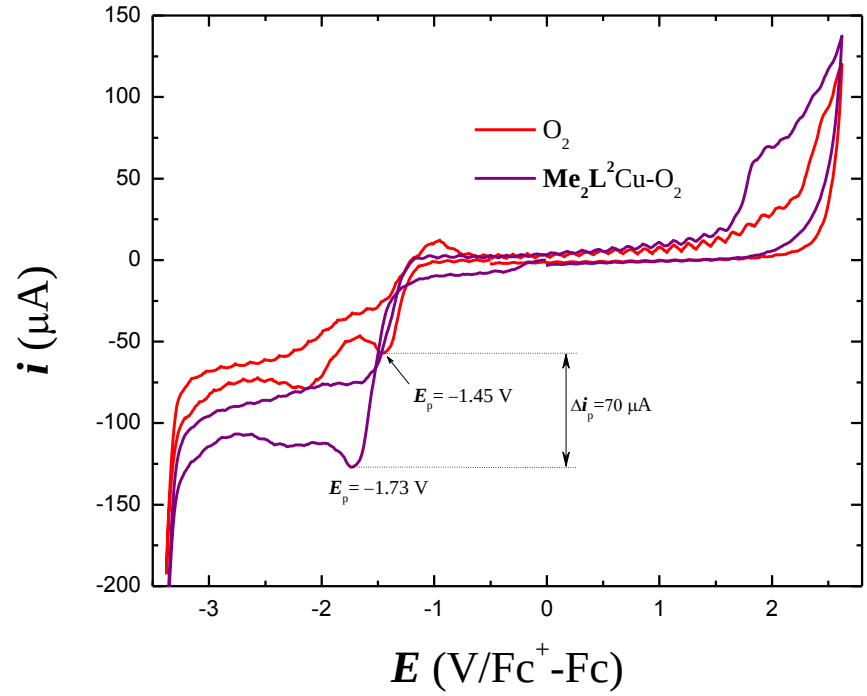

Figure S19. Representative voltammogram of 1 mM acetonitrile solution of $\mathbf{5}^{\mathbf{Me}}$ at –13°C with glassy carbon electrode (ϕ = 7.1 mm^2) and 0.1 M NBu_4PF_6 as supporting electrolyte: Reduction of O_2 (red line), reduction of $\mathbf{5}^{\mathbf{Me}}$ under O_2 (purple line).

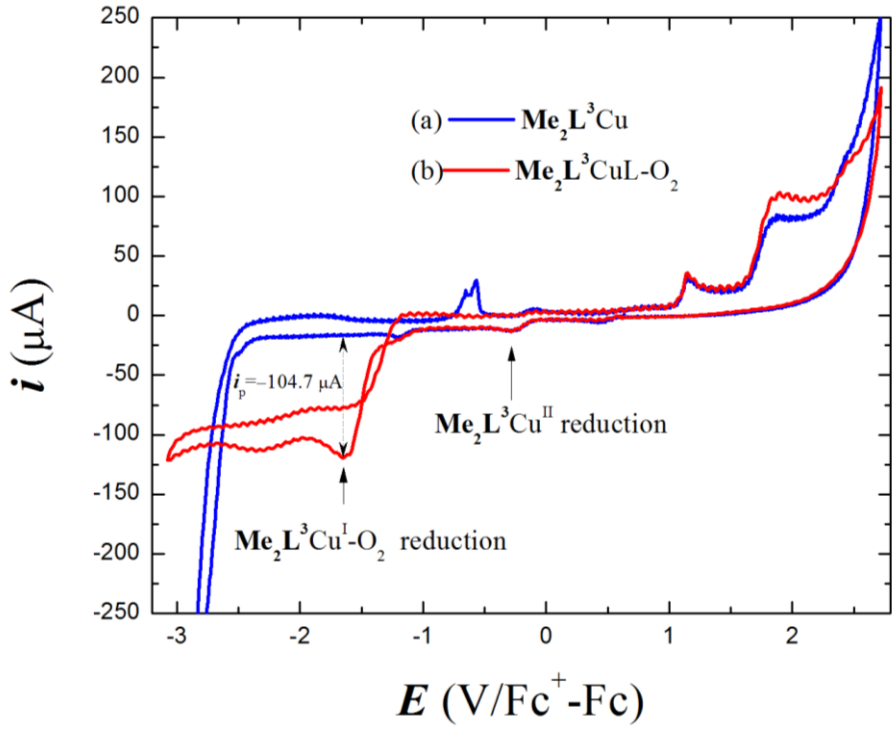

Figure S20. Representative cyclic voltammograms of 1 mM solutions of complex $\mathbf{6^{Me}}$ in 0.1 M Bu_4NPF_6 in acetonitrile at –13°C, measured with a glassy carbon electrode.

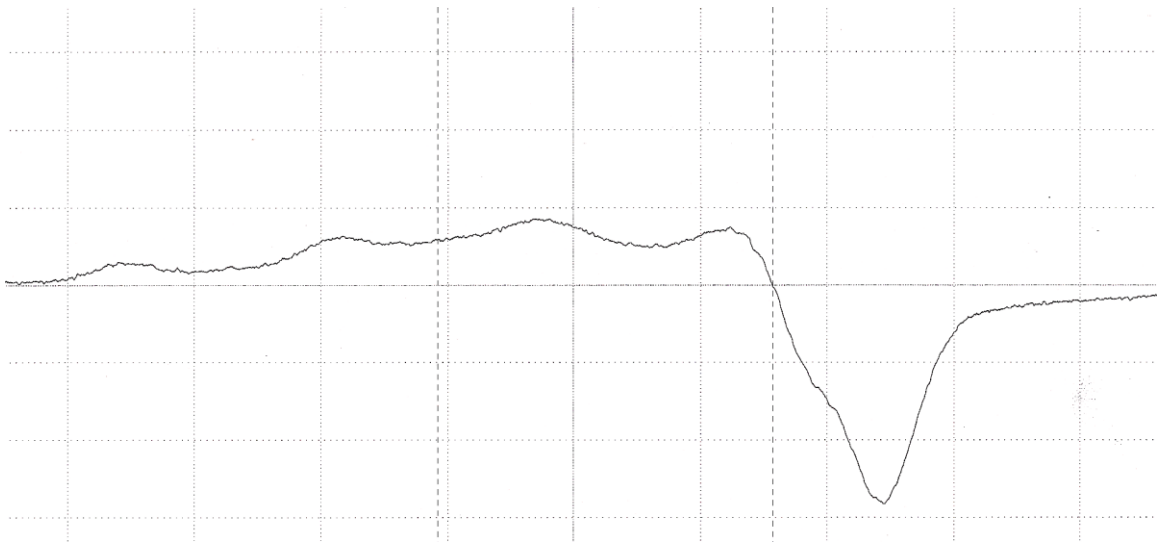

Figure S21. ESR spectrum of $\mathbf{5^{Me}}$ after exposure to O_2 for 1 h at -78°C in THF.

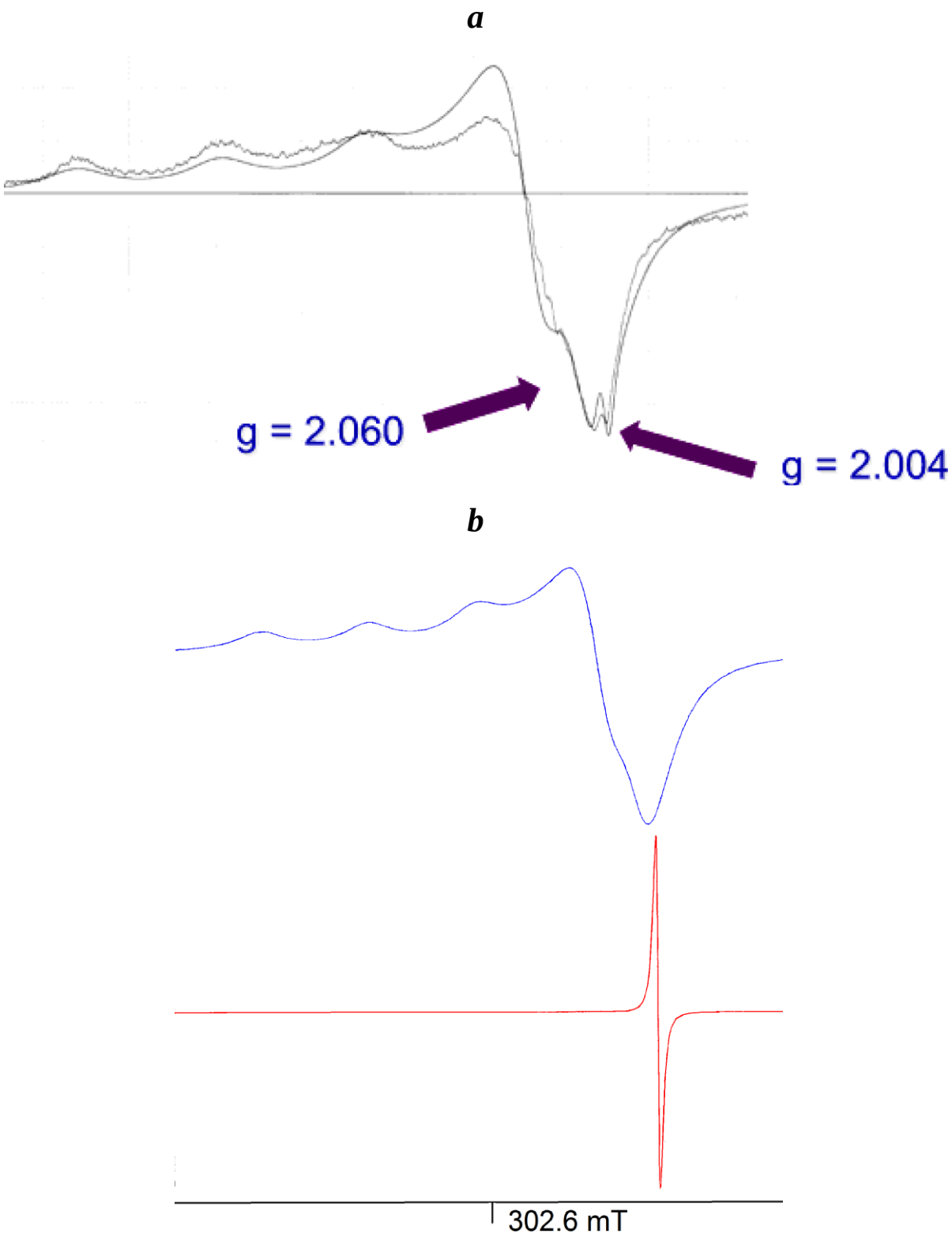

Figure S22. a) ESR spectrum and simulation of **6**^{Me} after exposure to O_2 for 1 h at -78°C in THF; b) Deconvoluted simulated spectra of Cu^{2+} complex and $O_2^{\cdot -}$.

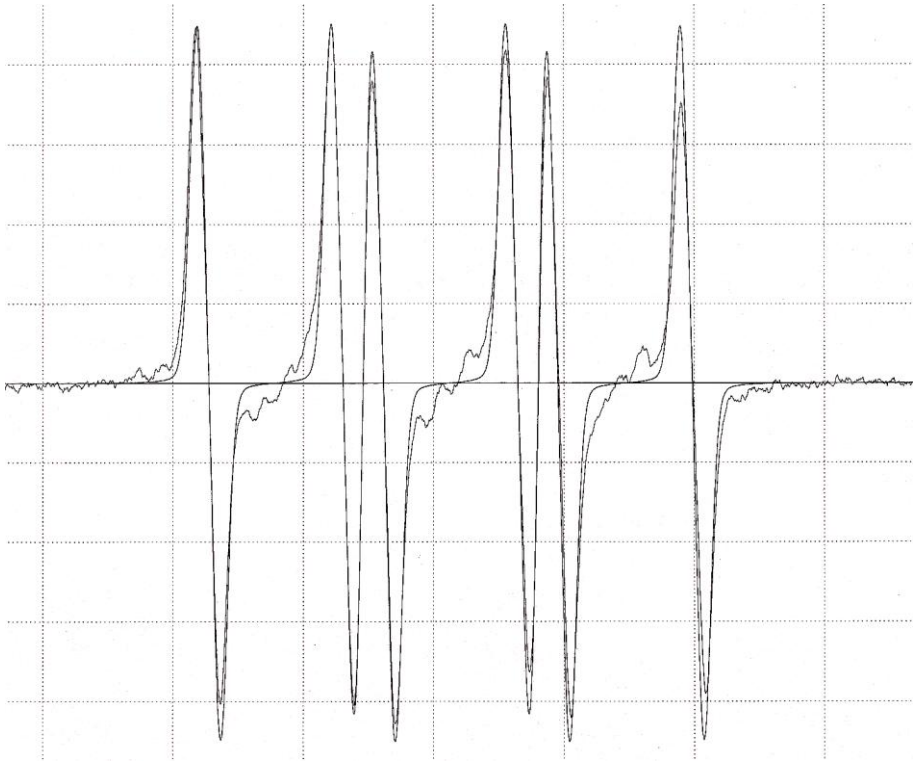

Figure S23. ESR spectrum and simulation of the DMPO-$O_2^{\bullet-}$ adduct obtained by oxygenation of $\mathbf{6^{Me}}$ in THF.